

# Analysis and Design of Launch Vehicle Flight Control Systems

Bong Wie\* and Wei Du<sup>†</sup>

*Iowa State University, Ames, IA 50011-2271*

*and*

Mark Whorton<sup>‡</sup>

*NASA Marshall Space Flight Center, Huntsville, AL 35812*

This paper describes the fundamental principles of launch vehicle flight control analysis and design. In particular, the classical concept of “drift-minimum” and “load-minimum” control principles is re-examined and its performance and stability robustness with respect to modeling uncertainties and a gimbal angle constraint is discussed. It is shown that an additional feedback of angle-of-attack or lateral acceleration can significantly improve the overall performance and robustness, especially in the presence of unexpected large wind disturbance. Non-minimum-phase structural filtering of “unstably interacting” bending modes of large flexible launch vehicles is also shown to be effective and robust.

## I. Introduction

**Note to Session Organizer/Reviewers:** This draft manuscript summarizes very preliminary results obtained during an early phase of a project for the launch vehicle flight control systems analysis and design as applied to Ares-I Crew Launch Vehicle. During the next several months, a more detailed, rigorous study will be conducted in the areas of drift-minimum vs load-minimum control, flexible-body stabilization and analysis, gain scheduling vs. adaptive control, etc. A companion paper on dynamic modeling of large flexible launch vehicles is also being submitted to this Space Exploration and Transportation GNC session.

## II. Rigid-Body Control Analysis

Consider a simplified linear dynamical model of a launch vehicle [15], as illustrated in Fig. 2, as follows:

$$\ddot{\theta} = M_{\alpha}\alpha + M_{\delta}\delta \quad (1)$$

$$\ddot{Z} = -\frac{F}{m}\theta - \frac{N_{\alpha}}{m}\alpha + \frac{T}{m}\delta \quad (2)$$

$$\alpha = \theta + \frac{\dot{Z}}{V} + \alpha_w \quad (3)$$

$$F = T_o + T - D \quad (4)$$

where  $\theta$  is the pitch attitude,  $\alpha$  the angle of attack,  $Z$  the inertial Z-axis drift position of the center-of-mass,  $\dot{Z}$  the inertial drift velocity,  $m$  the vehicle mass,  $T_o$  the ungimbaled sustainer thrust,  $T$  the gimbaled thrust,  $N = N_{\alpha}\alpha$  the aerodynamic normal (lift) force acting on the center-of-pressure,  $D$  the aerodynamic axial (drag) force,  $F$  the total

---

\*Vance Coffman Endowed Chair Professor, Space Systems and Controls Laboratory, Department of Aerospace Engineering, 2271 Howe Hall, Room 2355, (515) 294-3124, bongwie@iastate.edu, Associate Fellow AIAA.

<sup>†</sup>Ph.D. Student, Space Systems and Controls Laboratory, Department of Aerospace Engineering, Student Member AIAA.

<sup>‡</sup>Chief, Guidance, Navigation, and Mission Analysis Branch, mark.whorton@nasa.gov, Associate Fellow AIAA.

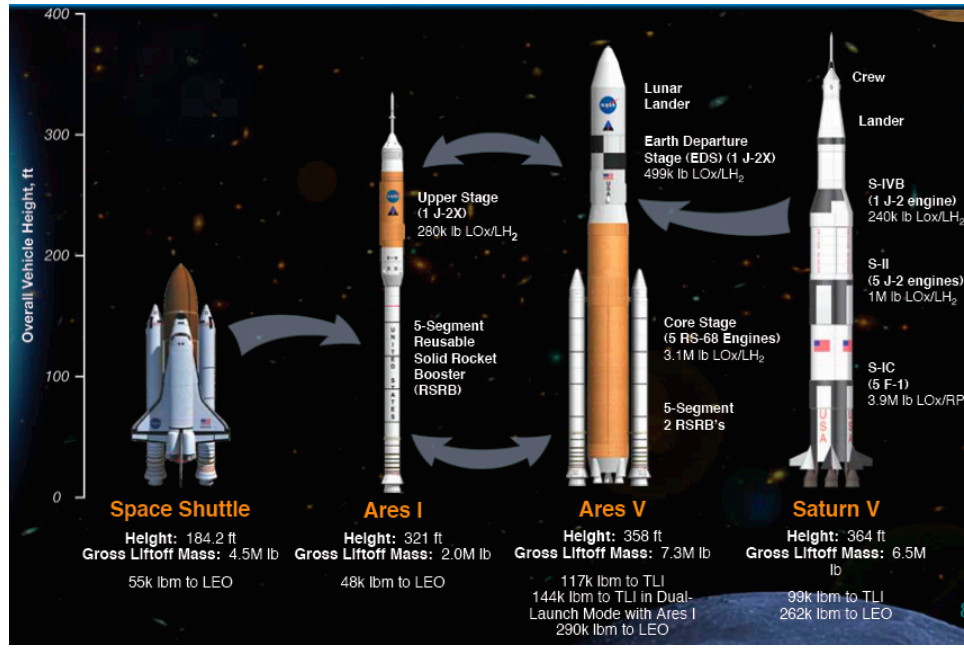


Figure 1. Comparison of Space Shuttle, Ares I, Ares V, and Saturn V Launch Vehicles [1].

x-axis force,  $\delta$  the gimbal deflection angle,  $V$  the vehicle velocity,  $\alpha_w = V_w/V$  the wind-induced angle of attack,  $V_w$  the wind disturbance velocity, and

$$M_\alpha = x_{cp} N_\alpha / I_y \quad (5)$$

$$M_\delta = x_{cg} T / I_y \quad (6)$$

$$N_\alpha = \frac{1}{2} \rho V^2 S C_{N_\alpha} \quad (7)$$

where  $I_y$  is the pitch moment of inertia. For an effective thrust vector control of a launch vehicle, we need

$$M_\delta \delta_{\max} > M_\alpha \alpha_{\max} \quad (8)$$

where  $\delta_{\max}$  is the gimbal angle constraint and  $\alpha_{\max}$  is the maximum wind-induced angle of attack.

The open-loop transfer functions from the control input  $\delta(s)$  can then be obtained as

$$\frac{\theta(s)}{\delta(s)} = \frac{s}{\Delta(s)} \left[ M_\delta \left( s + \frac{N_\alpha}{mV} \right) + \frac{M_\alpha T}{mV} \right] \quad (9)$$

$$\frac{Z(s)}{\delta(s)} = \frac{1}{\Delta(s)} \left[ \frac{T}{m} (s^2 - M_\alpha) - \frac{M_\alpha (F + N_\alpha)}{m} \right] \quad (10)$$

$$\frac{\alpha(s)}{\delta(s)} = \frac{s}{\Delta(s)} \left[ \frac{T}{mV} s^2 - M_\delta s + \frac{M_\delta F}{mV} \right] \quad (11)$$

where

$$\Delta(s) = s \left[ s^3 + \frac{N_\alpha}{mV} s^2 - M_\alpha s + \frac{M_\alpha F}{mV} \right] \quad (12)$$

Consequently, the 4th-order system described by Eq. (1) - (3) is completely controllable by  $\delta$  and is observable by  $Z$ ; however, the system is not observable by  $\theta$  and  $\alpha$ .

In 1959, Hoelkner introduced the “drift-minimum” and “load-minimum” control concepts as applied to the launch vehicle flight control system [6]. The concepts have been further investigated in [7-14]. Basically, Hoelkner’s controller utilizes a full-state feedback control of the form

$$\delta = -K_1 \theta - K_2 \dot{\theta} - K_3 \alpha \quad (13)$$

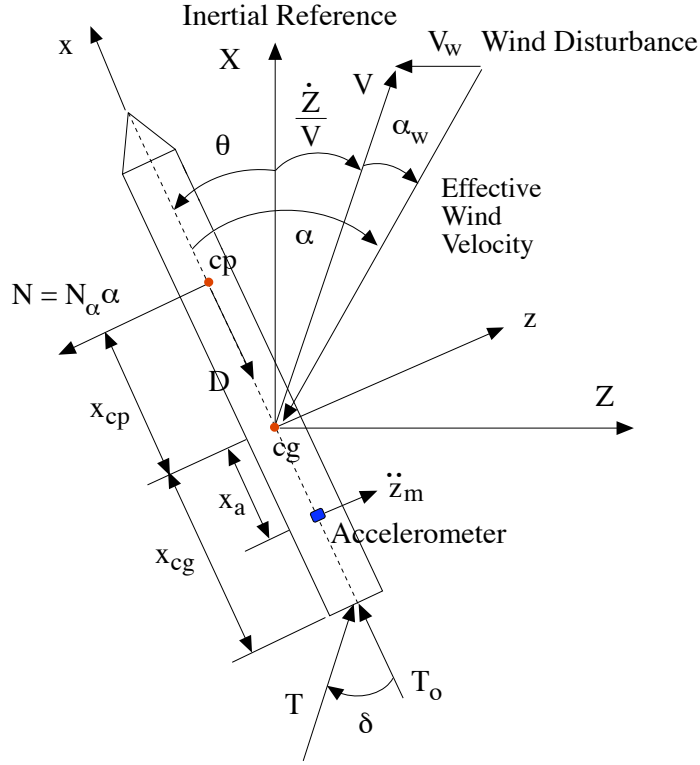


Figure 2. Simplified pitch-axis model of a launch vehicle.

for a 3rd-order dynamical model of the form

$$\frac{d}{dt} \begin{bmatrix} \theta \\ \dot{\theta} \\ \alpha \end{bmatrix} = \begin{bmatrix} 0 & 1 & 0 \\ 0 & 0 & M_\alpha \\ -F/(mV) & 1 & -N_\alpha/(mV) \end{bmatrix} \begin{bmatrix} \theta \\ \dot{\theta} \\ \alpha \end{bmatrix} + \begin{bmatrix} 0 \\ M_\delta \\ T/(mV) \end{bmatrix} \delta + \begin{bmatrix} 0 \\ 0 \\ \dot{\alpha}_w \end{bmatrix} \quad (14)$$

This 3rd-order system is observable by  $\theta$  or  $\alpha$ . The feedback gains are to be properly selected to minimize the lateral drift velocity  $\dot{Z} = V(\alpha - \theta - \alpha_w)$  or the bending moment caused by the angle of attack. Note that

$$\frac{\dot{Z}}{V} \equiv \gamma = \alpha - \theta - \alpha_w \quad (15)$$

where  $\gamma$  is often called the flight-path angle.

Instead of measuring the angle-of-attack, we may employ a body-mounted accelerometer, as illustrated in Fig. 2, as follows:

$$\begin{aligned} \delta &= -K_1\theta - K_2\dot{\theta} + K_a\ddot{z}_m \\ &= -K_1\theta - K_2\dot{\theta} + K_a \left( -\frac{N_\alpha}{m}\alpha + \frac{T}{m}\delta + \frac{x_a}{m}\ddot{\theta} \right) \\ &= -K_1\theta - K_2\dot{\theta} + K_a\frac{x_a}{m}\ddot{\theta} - K_a\frac{N_\alpha}{m}\alpha + K_a\frac{T}{m}\delta \end{aligned}$$

Because the resulting effect of  $\ddot{z}_m$  feedback is basically the same as the  $\alpha$  feedback, we consider here only the control logic described by Eq. (13).

Substituting Eq. (13) into Eq. (1) - (2) or Eq. (14), we obtain the closed-loop transfer function from the wind disturbance  $\alpha_w(s)$  to the drift velocity  $\dot{Z}(s)$  as

$$\frac{\dot{Z}}{\alpha_w V} = -\frac{A_2 s^2 + A_1 s + A_o}{s^3 + B_2 s^2 + B_1 s + B_o} \quad (16)$$

where

$$\begin{aligned}
B_2 &= M_\delta K_2 + \frac{T}{mV} \left( K_3 + \frac{N_\alpha}{T} \right) \\
B_1 &= M_\delta (K_1 + K_3) - M_\alpha + \frac{K_2 T}{mV} \left( M_\alpha + \frac{M_\delta N_\alpha}{T} \right) \\
B_o &= \frac{TK_1}{mV} \left( M_\alpha + \frac{M_\delta N_\alpha}{T} \right) - \frac{F}{mV} (M_\delta K_3 - M_\alpha) \\
A_2 &= \frac{T}{mV} \left( K_3 + \frac{N_\alpha}{T} \right) \\
A_1 &= \frac{K_2 T}{mV} \left( M_\alpha + \frac{M_\delta N_\alpha}{T} \right) \\
A_o &= B_o
\end{aligned}$$

For a unit-step wind disturbance of  $\alpha_w(s) = 1/s$ , the steady-state value of  $\dot{Z}$  can be found as

$$\frac{\dot{Z}_{ss}}{V} = \lim_{s \rightarrow 0} \frac{-(A_2 s^2 + A_1 s + A_o)}{s^3 + B_2 s^2 + B_1 s + B_o} = \frac{-A_o}{B_o} = -1 \quad (17)$$

The launch vehicle drifts along the wind direction with  $\dot{Z}_{ss} = -V_w$  and also with  $\theta = \dot{\theta} = \alpha = \delta = 0$  as  $t \rightarrow \infty$ . It is interesting to notice that the steady-state drift velocity (or the flight path angle) is independent of feedback gains provided an asymptotically stable closed-loop system with  $B_o \neq 0$ .

If we choose the control gains such that  $B_o = 0$  (i.e., one of the closed-loop system roots is placed at  $s = 0$ ), the steady-state value of  $\dot{Z}$  becomes

$$\frac{\dot{Z}_{ss}}{V} = \lim_{s \rightarrow 0} \frac{-(A_2 s + A_1)}{s^2 + B_2 s + B_1} = \frac{-A_1}{B_1} = \frac{-1}{1+C} \quad (18)$$

where

$$C = \frac{mV[M_\delta(K_1 + K_3) - M_\alpha]}{M_\alpha K_2 T + M_\delta N_\alpha / T} \quad (19)$$

For a stable closed-loop system with  $M_\delta(K_1 + K_3) - M_\alpha > 0$ , we have  $C > 1$  and

$$|\dot{Z}_{ss}| < V_w \quad (20)$$

when  $B_o = 0$ . The drift-minimum condition,  $B_o = 0$ , can be rewritten as

$$\frac{M_\delta K_3 - M_\alpha}{M_\delta K_1} = \frac{N_\alpha}{F} \left( 1 + \frac{x_{cp}}{x_{cg}} \right) \quad (21)$$

Consider the following closed-loop transfer functions:

$$\frac{\alpha}{\alpha_w} = -\frac{s(s^2 + M_\delta K_2 s + M_\delta K_1)}{s^3 + B_2 s^2 + B_1 s + B_o} \quad (22)$$

$$\frac{\delta}{\alpha_w} = -\frac{s(K_3 s^2 + M_\alpha K_2 s + M_\alpha K_1)}{s^3 + B_2 s^2 + B_1 s + B_o} \quad (23)$$

For a unit-step wind disturbance of  $\alpha_w(s) = 1/s$ , we have  $\alpha = \delta = 0$  as  $t \rightarrow \infty$ . However, for a unit-ramp wind disturbance of  $\alpha_w(s) = 1/s^2$ , we have

$$\begin{aligned}
\lim_{t \rightarrow \infty} \alpha(t) &= M_\delta K_1 \\
\lim_{t \rightarrow \infty} \delta(t) &= M_\alpha K_1
\end{aligned}$$

Consequently, the bending moment induced by  $\alpha$  and  $\delta$  can be minimized by choosing  $K_1 = 0$ , which is the “load-minimum” condition introduced by Hoelkner [6]. The closed-loop system with  $K_1 = 0$  is unstable because

$$B_o = -\frac{F}{mV} (M_\delta K_3 - M_\alpha) < 0 \quad (24)$$

However, the load-minimum control for short durations has been known to be acceptable provided a deviation from the nominal flight trajectory is permissible.

A set of full-state feedback control gains,  $(K_1, K_2, K_3)$ , can be found by using a pole-placement approach or the linear-quadratic-regulator (LQR) control method [21-22], as follows:

$$\min_{\delta} \int_0^{\infty} (x^T Q x + \delta^2) dt \quad (25)$$

subject to  $\dot{x} = Ax + B\delta$  and  $\delta = -Kx$  where  $x = [\theta \ \dot{\theta} \ \alpha]^T$  and  $K = [K_1 \ K_2 \ K_3]$ .

### III. Rigid-Body Control Example

Consider a launch vehicle control design example discussed by Greensite in [15]. Its basic parameters are given as in [15]

$$\begin{aligned} I_y &= 2.43E6 \text{ slug-ft}^2, & m &= 5830 \text{ slug}, & T &= 341,000 \text{ lb} \\ F &= 375,000 \text{ lb}, & x_{cp} &= 38 \text{ ft}, & x_{cg} &= 32.3 \text{ ft} \\ V &= 1320 \text{ ft/sec}, & V_w &= 132 \text{ ft/sec}, & \alpha_w &= 5.73 \text{ deg} \\ N_{\alpha} &= 240,000 \text{ lb/rad}, & M_{\alpha} &= 3.75 \text{ s}^{-2}, & M_{\delta} &= 4.54 \text{ s}^{-2} \end{aligned} \quad (26)$$

The open-loop poles of this example vehicle are: -1.9767, 0.0488, 1.8967

Note that the wind-induced angle of attack of 5.73 deg considered for this example in [15] is somewhat unrealistic because it will require a maximum gimbal deflection angle of

$$\delta_{\max} > \frac{M_{\alpha}}{M_{\delta}} \alpha_w = 4.73 \text{ deg}$$

Most practical thrust vector control systems have a maximum gimbal angle constraint of about  $\pm 5$  deg. In this paper, we also assume a second-order gimbal actuator dynamics of the form

$$\delta(s) = \frac{\omega_n^2}{s^2 + 2\zeta\omega_n s + \omega_n^2} \delta_c(s) \quad (27)$$

where  $\zeta = 1$  and  $\omega_n = 50 \text{ rad/s}$ .

**Table 1. Summary of rigid-body control analysis and design**

Case No.	Controller Type	Feedback Gains $(K_1, K_2, K_3)$	Closed-Loop Poles
1	$(\theta, \dot{\theta})$ -Feedback Control [15]	(2, 0.8, 0)	-1.7488±1.3934j, -0.1596
2	Drift-Minimum Control [15]	(2, 0.8, 3.614)	-1.9087±4.2774j, 0.0
3	Load-Minimum Control [15]	(0, 0.8, 3.614)	-1.9323±3.0533j, 0.0471
4	LQR Control (Q = 0)	(0.6852, 0.8491, 0.9542)	-1.9767, -1.8967, -0.0488
5	Drift-Minimum Control	(0.3220, 0.8352, 1.2765)	-1.9767, -1.8967, 0.0
6	Load-Minimum Control	(0, 0.8352, 1.2765)	-3.1323, -0.7816, 0.0405

### IV. Flexible-Body Control Analysis

More detailed control and stability analysis results for Figs. 10 and 11 will be included in the final manuscript.

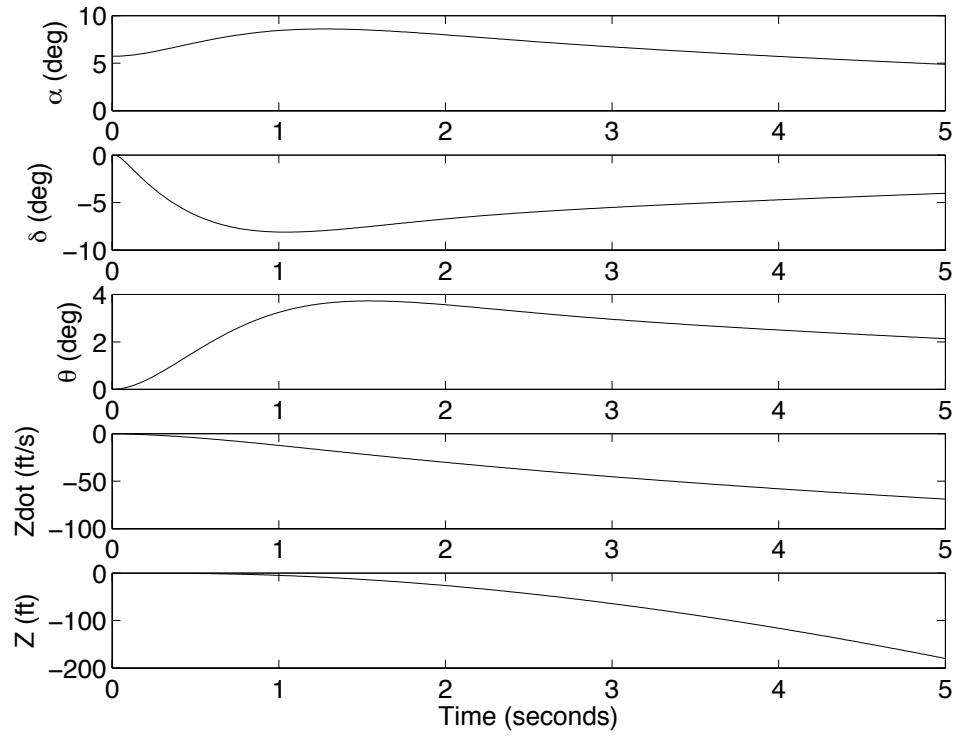


Figure 3.  $(\theta, \dot{\theta})$ -feedback control (Case 1).

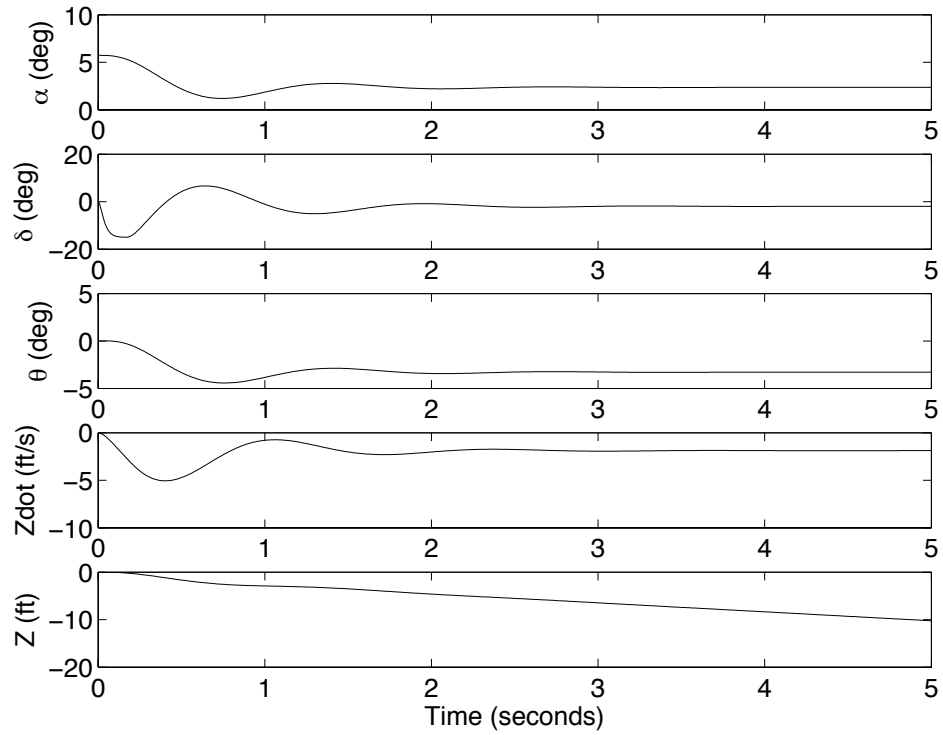


Figure 4. Drift-minimum control (Case 2).

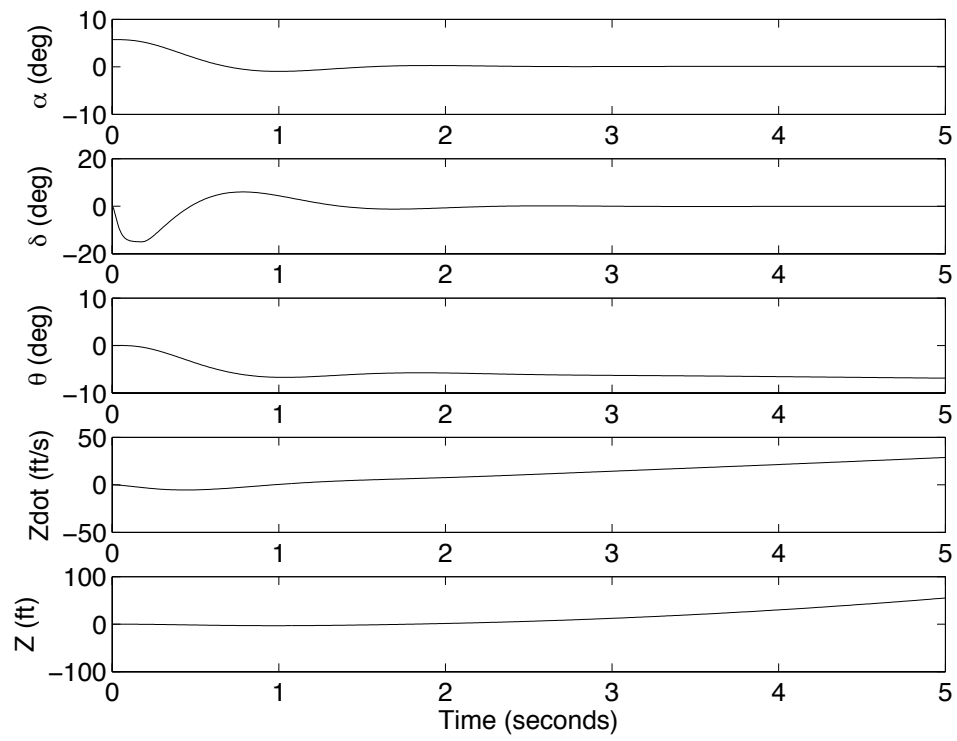


Figure 5. Load-minimum control (Case 3).

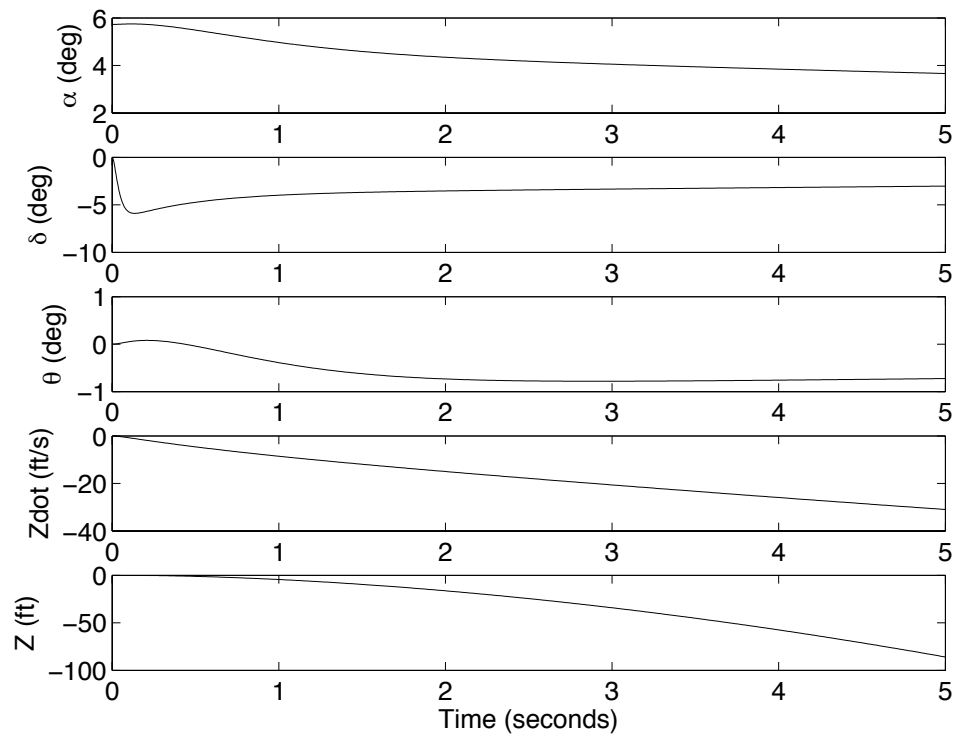


Figure 6. LQR control (Case 4).

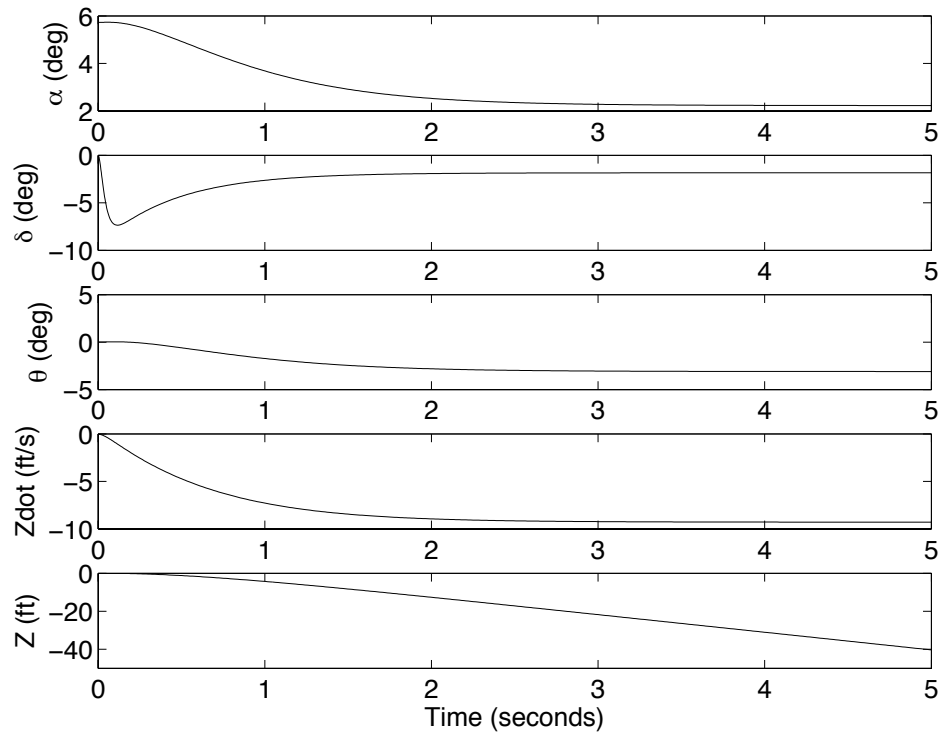


Figure 7. Drift-minimum control (Case 5).

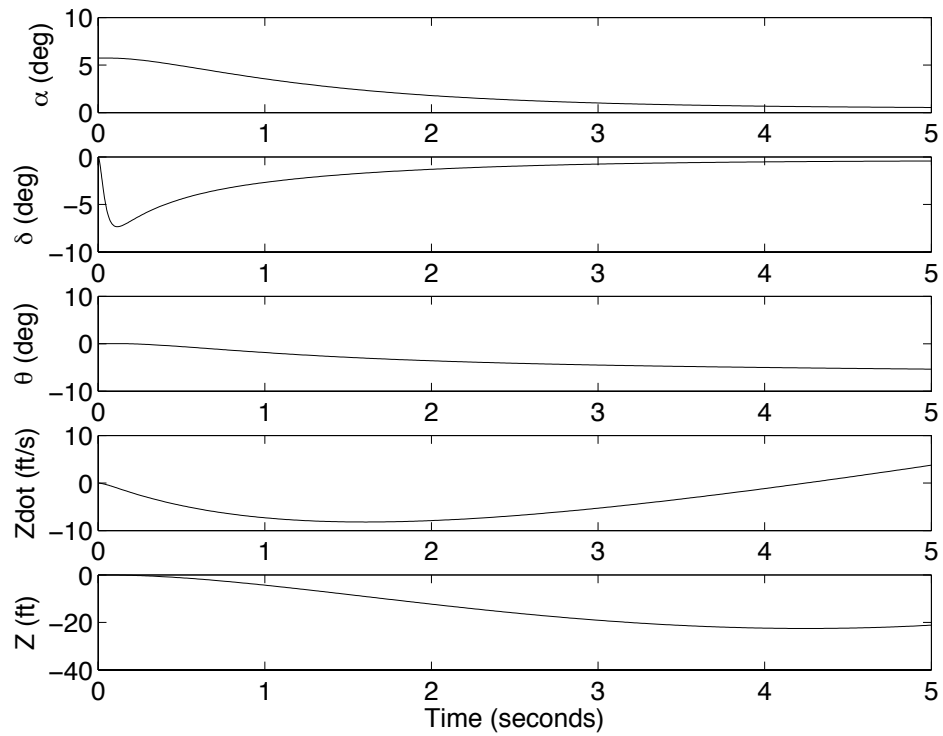


Figure 8. Load-minimum control (Case 6).



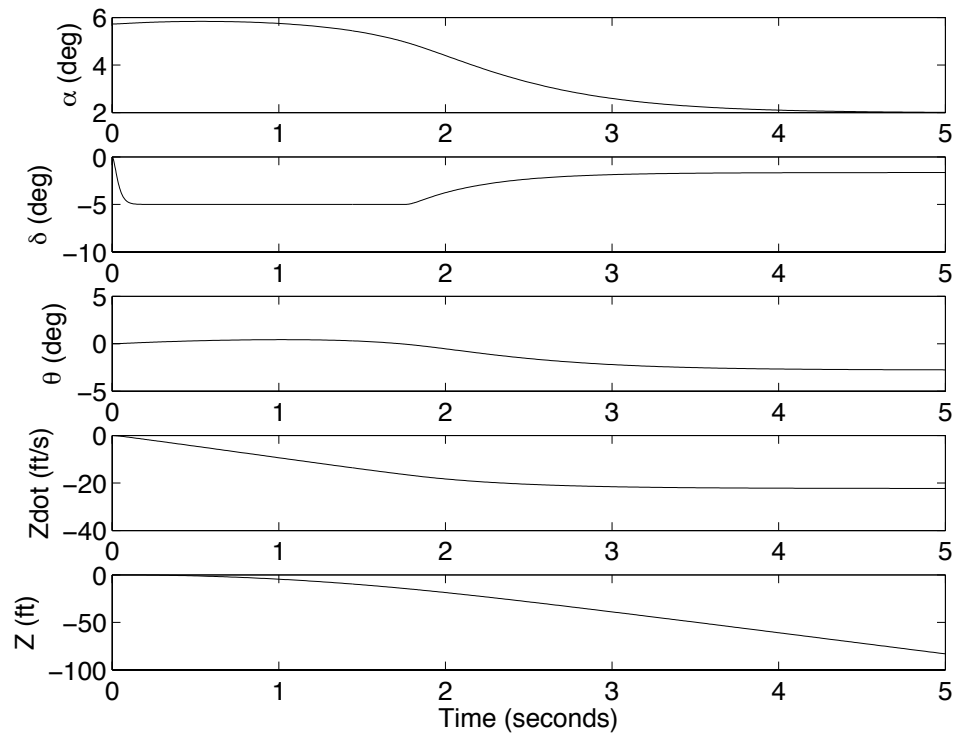


Figure 9. Case 5 (drift-minimum control) with  $\delta_{\max} = \pm 5$  deg.

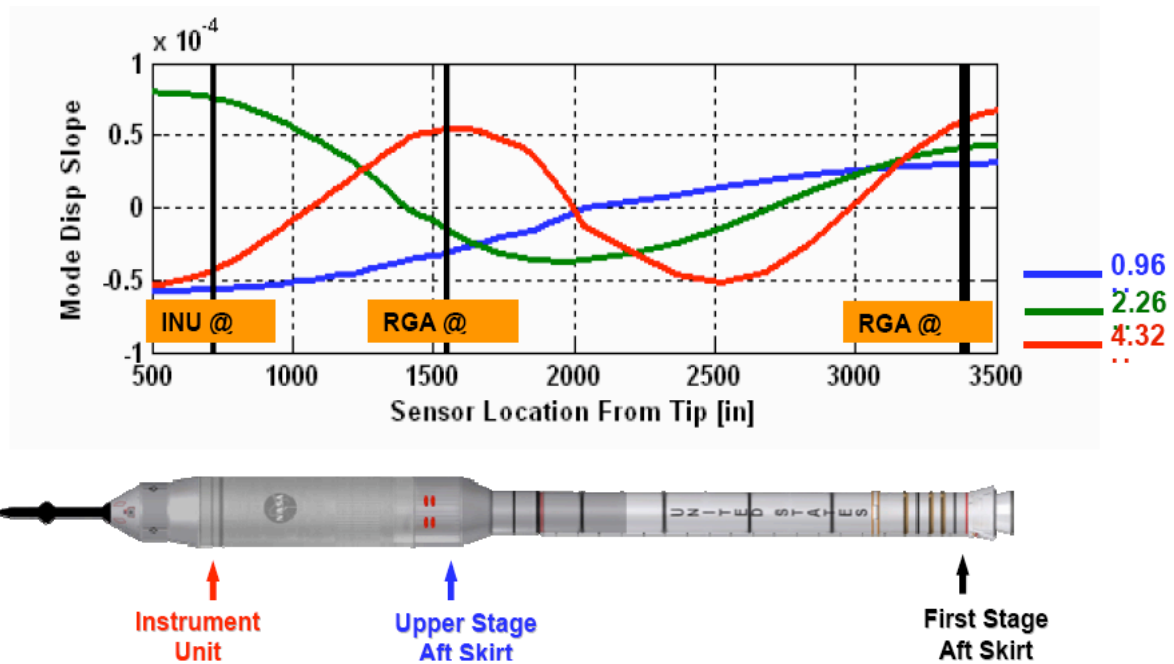


Figure 10. Illustrations of dominant bending modes and sensor locations (Ref. 2).

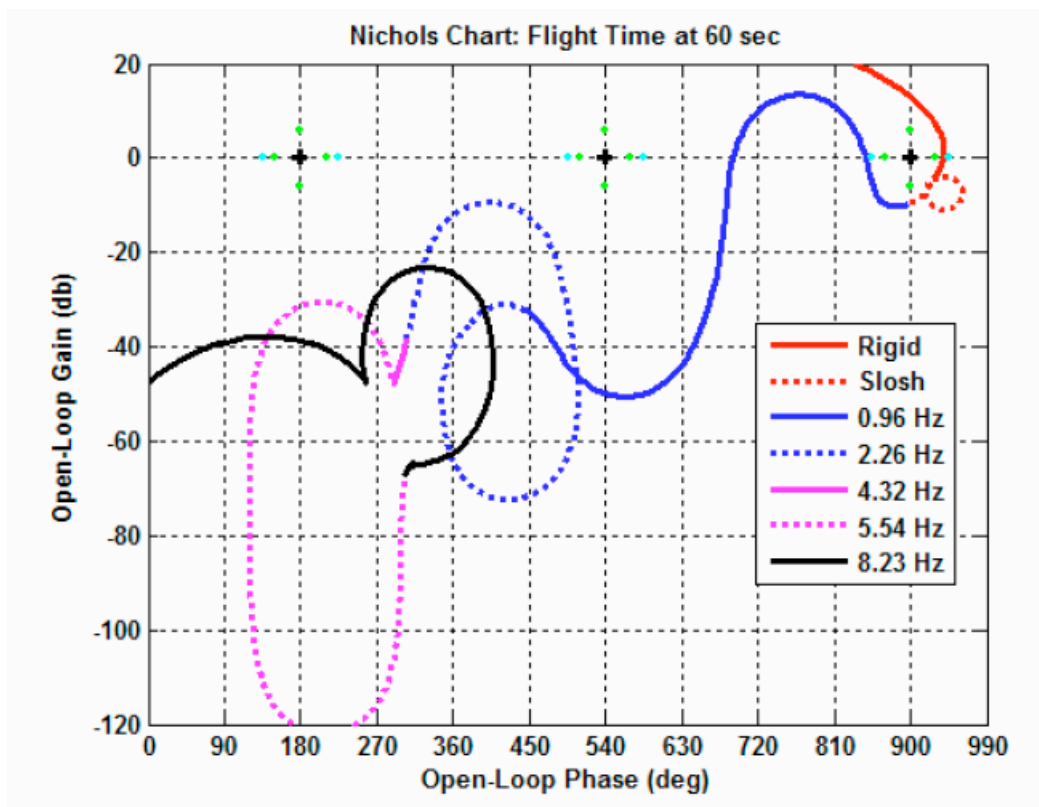


Figure 11. Nichols plot for a baseline pitch-axis flight control system (Ref. 2).

## V. Conclusions

## References

- [1] Cook, S., "Ares Project Status," Presented at *2nd AIAA Space Exploration Conference*, December 4-6, 2006.
- [2] Whorton, M., Hall, C., and Cook, S., "Ascent Flight Control and Structural Interaction for the Ares-I Crew Launch Vehicle," AIAA 2007-1780, April 2007.
- [3] Jang, J.-W., Bedrossian, N., Hall, R., Norris, H., Hall, C., and Jackson, M., "Initial Ares-I Bending Filter Design," AAS 07-059, February 2007.
- [4] Betts, K. M., Rutherford, R. C., McDuffie, J., Johnson, M. D., Jackson, M., and Hall, C., "Time Domain Simulation of the NASA Crew Launch Vehicle," AIAA 2007-6621, August 2007.
- [5] Betts, K. M., Rutherford, R. C., McDuffie, J., Johnson, M. D., Jackson, M., and Hall, C., "Stability Analysis of the NASA ARES I Crew Launch Vehicle Control System," AIAA 2007-6776, August 2007.
- [6] Hoelkner, R. F., "The Principle of of Artificial Stabilization of Aerodynamically Unstable Missiles," ABMA DA-TR-64-59, September 25, 1959.
- [7] Hoelkner, R. F., "Theory of Artificial Stabilization of Missiles and Space Vehicles with Exposition of Four Control Principles," NASA TN D-555, June 1961.
- [8] Harris, R. J., "Trajectory Simulation Applicable to Stability and Control Studies of Large Multi-Engine Vehicles," NASA TN D-1838, August 1963.
- [9] Harvey, C. A., "An Alternate Derivation and Interpretation of the Drift-Minimum Principle," NASA Contract NASw-563, MH MPG Report 1541-TR 15, Minneapolis-Honeywell, November 22, 1963.
- [10] Garner, D., "Control Theory Handbook," NASA TM X-53036, April 22, 1964.
- [11] Rheinfurth, M. H., "The Alleviation of Aerodynamic Loads on Rigid Space Vehicles," NASA TM X-53397, February 21, 1966.
- [12] Martin, D. T., Sievers, R. F., O'Brien, R. M., and Rice, A. F., "Saturn V Guidance, Navigation, and Targeting," *J. Spacecraft*, Vol. 4, No. 7, 1967, pp. 891-898.
- [13] Frosch, J. A. and Valley, D. P., "Saturn AS-501/S-IC Flight Control System Design," *J. Spacecraft*, Vol. 4, No. 8, 1967, pp. 1003-1009.
- [14] Haeussermann, W., "Description and Performance of the Saturn Launch Vehicle's Navigation, Guidance, and Control System," NASA TN D-5869, July 1970.
- [15] Greensite, A. L., "Analysis and Design of Space Vehicle Flight Control Systems," Spartan Books, New York, 1970.
- [16] Blackburn, T. R. and Vaughan, D. R., "Application of Linear Optimal Control and Filtering Theory to the Saturn V Launch Vehicle," *IEEE Transactions on Automatic Control*, Vol. AC-16, No. 6, Dec. 1971, pp. 799-806.
- [17] Wie, B., "Thrust Vector Control Design for a Liquid Upper Stage Spacecraft," *Journal of Guidance, Control, and Dynamics*, Vol. 8, No. 5, 1985, pp. 566-572.
- [18] Wie, B. and Byun, K. W., "New Generalized Structural Filtering Concept for Active Vibration Control Synthesis," *Journal of Guidance, Control, and Dynamics*, Vol. 12, No. 2, 1989, pp. 147-154.
- [19] Byun, K. W., Wie, B. and Sunkel, J., "Robust Non-Minimum-Phase Compensation for a Class of Uncertain Dynamical Systems," *Journal of Guidance, Control, and Dynamics*, Vol. 14, No. 6, 1991, pp. 1191-1199.
- [20] Wie, B., Liu, Q. and Bauer, F., "Classical and Robust  $H_\infty$  Control Redesign for the Hubble Space Telescope," *Journal of Guidance, Control, and Dynamics*, Vol. 16, No. 6, 1993, pp. 1069-1077.
- [21] Bryson, A. E., *Control of Spacecraft and Aircraft*, Princeton University Press, 1994.
- [22] Bryson, A. E., *Applied Linear Optimal Control*, Cambridge University Press, 2002.
- [23] Wie, B., *Space Vehicle Dynamics and Control*, AIAA Education Series, 1998.